

## ARTICLE

# Dystroglycan is essential for early embryonic development: disruption of Reichert's membrane in *Dag1*-null mice

Roger A. Williamson<sup>1,§</sup>, Michael D. Henry<sup>2,§</sup>, Karla J. Daniels<sup>3</sup>, Ronald F. Hrstka<sup>1</sup>, Jane C. Lee<sup>2</sup>, Yoshihide Sunada<sup>2</sup>, Oxana Ibraghimov-Beskrovnaya<sup>2,+</sup> and Kevin P. Campbell<sup>2,\*</sup>

<sup>1</sup>Department of Obstetrics and Gynecology, University of Iowa Hospitals and Clinics, Iowa City, IA 52242, USA,

<sup>2</sup>Howard Hughes Medical Institute, Department of Physiology and Biophysics, University of Iowa College of Medicine, Iowa City, IA 52242, USA and <sup>3</sup>Department of Biological Sciences, University of Iowa, Iowa City, IA 52242, USA

Received December 23, 1996; Revised and Accepted March 7, 1997

DDBJ/EMBL/GenBank accession no. U48854

**Dystroglycan is a central component of the dystrophin–glycoprotein complex (DGC), a protein assembly that plays a critical role in a variety of muscular dystrophies. In order to better understand the function of dystroglycan in development and disease, we have generated a null allele of dystroglycan (*Dag1<sup>neo2</sup>*) in mice. Heterozygous *Dag1<sup>neo2</sup>* mice are viable and fertile. In contrast, homozygous *Dag1<sup>neo2</sup>* embryos exhibit gross developmental abnormalities beginning around 6.5 days of gestation. Analysis of the mutant phenotype indicates that an early defect in the development of homozygous *Dag1<sup>neo2</sup>* embryos is a disruption of Reichert's membrane, an extra-embryonic basement membrane. Consistent with the functional defects observed in Reichert's membrane, dystroglycan protein is localized in apposition to this structure in normal egg cylinder stage embryos. We also show that the localization of two critical structural elements of Reichert's membrane—laminin and collagen IV—are specifically disrupted in the homozygous *Dag1<sup>neo2</sup>* embryos. Taken together, the data indicate that dystroglycan is required for the development of Reichert's membrane. Furthermore, these results suggest that disruption of basement membrane organization might be a common feature of muscular dystrophies linked to the DGC.**

## INTRODUCTION

Dystroglycan was first identified in skeletal muscle as a component of the dystrophin–glycoprotein complex (DGC) (1). It is composed of  $\alpha$ - and  $\beta$ -subunits which are post-translationally derived from a single mRNA species encoded by a single gene (2,3). In skeletal muscle,  $\alpha$ -dystroglycan is an extracellular peripheral membrane glycoprotein that binds to laminin-2 in the extracellular matrix (4) and  $\beta$ -dystroglycan is an integral membrane glycoprotein that anchors  $\alpha$ -dystroglycan to the membrane (5) and binds intracellularly to dystrophin which is associated with the F-actin cytoskeleton (6,7). Thus, dystroglycan spans the sarcolemma providing a connection between the extracellular matrix and the cytoskeleton (8). Mutations in genes encoding a number of DGC components disrupt this dystroglycan-mediated linkage and lead to various forms of muscular dystrophy in humans and in mice (9). Together, these biochemical and genetic data have suggested that

the connection between the extracellular matrix and the cytoskeleton provided by dystroglycan serves to stabilize the sarcolemma during contraction-induced stress. However, to date, no form of muscular dystrophy has been linked to the dystroglycan gene itself.

Skeletal muscle dystroglycan is also localized to the neuromuscular junction (10) where  $\alpha$ -dystroglycan binds to agrin (11). These findings led to considerable speculation that dystroglycan mediated agrin-induced acetylcholine-receptor clustering during development of the neuromuscular junction. Two studies independently demonstrated that an anti-dystroglycan antibody preparation impaired agrin-induced acetylcholine receptor clustering in cultured myotubes (12,13). However, it was subsequently shown that  $\alpha$ -dystroglycan binds to both cluster-inducing neural agrin and non-inducing muscle agrin isoforms (14). Moreover, the domain of agrin responsible for acetylcholine

\*To whom correspondence should be addressed. Tel: +1 319 335 7867; Fax: +1 319 335 6957; Email: kevin-campbell@uiowa.edu

+Present address: Genzyme Genetics, Framingham, MA 01701, USA

§Both authors contributed equally to this work

receptor clustering is physically separable from the domain that binds to dystroglycan (15). These latter studies suggest it is unlikely that dystroglycan is directly transducing the signal from agrin that initiates the clustering of acetylcholine receptors. Therefore, dystroglycan's role in the development of the neuromuscular junction remains unclear.

Unlike some of the other components of the DGC, dystroglycan is expressed in a broad array of adult tissues (2,3). Dystroglycan's function in these non-muscle tissues is largely unknown, although in some cases its function has been inferred from its subcellular localization. For instance, localization of dystroglycan to the perivascular endfeet of glial cells has suggested that it might play a role in maintenance of the blood-brain barrier (16). Dystroglycan function has been directly tested thus far in only one non-muscle tissue, the developing kidney. Utilizing an organ culture system, Durbeej *et al.* showed that a function-blocking anti-dystroglycan antibody disrupted kidney epithelial morphogenesis (17). However, dystroglycan's exact role in this complex developmental process is not yet understood.

We sought to better understand the function of dystroglycan by targeted disruption of its gene in the mouse. Our results indicate that dystroglycan is required for the development of Reichert's membrane, one of the first basement membranes that form during murine development. Taken together, the data suggest that dystroglycan may be necessary for the assembly of the extracellular matrix proteins that comprise Reichert's membrane. Elucidation of such an extracellular matrix assembly function for dystroglycan could have significant impact in understanding its involvement in muscular dystrophy and other developmental processes.

**RESULTS**

**Isolation and expression of the mouse dystroglycan gene (*Dag1*)**

We isolated *Dag1* from a 129/SvJ mouse genomic library by screening with a radiolabeled human dystroglycan cDNA probe. Translation of the putative coding sequence from this genomic clone reveals that murine dystroglycan shares a high degree (94%) of amino acid sequence identity with human dystroglycan (Fig. 1). Furthermore, comparison of the mouse dystroglycan genomic sequence with the human genomic sequence indicates that the organization of the dystroglycan gene into two exons is also conserved between mouse and man (data not shown). Northern blot analysis reveals the presence of a single 5.8 kb transcript in mRNA preparations of whole embryos between 7 and 17 days of gestation (Fig. 2A). In the adult mouse, dystroglycan mRNA is detectable in a wide variety of tissues (Fig. 2B). Both the size of the dystroglycan transcript and its broad tissue distribution are consistent with previous studies in rabbit (2) and human (3).

**Generation and analysis of *Dag1*-null animals**

We generated the *Dag1<sup>neo2</sup>* allele in embryonic stem (ES) cells by the gene targeting strategy depicted in Figure 3. Approximately 1 in 70 ES cell colonies surviving drug selection were appropriately targeted (Fig. 3B). Chimeric mouse embryos were produced by aggregating targeted ES cells with zona-denuded morulae which had been frozen at the 2-cell stage

mouse	MSVDNWLHLPLWGQTFLLLSVAVAQAHPSEPESEAVRDWKNQLEASM	48
human	MR***GLS**L***R*****VM*****E*****	
		†
mouse	HSVLSDFQEAAPTAVVGI PDGTAVVGRSFRVSIPTDLLASSGELIKVSAAG	98
human	*****LH*****T*****D*****	
		†
mouse	KEALPSWLHWDPHSHILEGLPLDITDKGVHYISVSAARLGGANGSHVPTSS	148
human	*****SQ**T*****I*****	
mouse	VFSIEVYPEDHNEPQSVRAASSDPGEVVPSCAADEPVTVLTVILDADLT	198
human	*****SDL***T**P*****S*****I*****	
mouse	KMTPKQRIDLLNRMQSFSEVELHNMKLVVNNRFLDMSAFMAGPNAKK	248
human	*****H**R*****P**	
mouse	VVENGALLSWKLGCSLNQNSVPDIRGVETPAREGAMSAQLGYVVGWHIA	298
human	*****H***A*****	
mouse	NKKPTLPKRLRRQIHATPTPVTAIGPPTTAIQEPPSRIVPTPTSPIAAPP	348
human	***p***V*****I*****	
mouse	TETMAPFVRDPVPGKPTVITIRGAI IQTPTLGP IQPTRVSEAGTTVPGQ	398
human	*****I*****	
mouse	IRPTLTIPGYVEPTAVITPPTTTTKKPRVSTPKPATPSTDSSTTTTTRRPT	448
human	***M*****A*****T*****	
		†
mouse	KKPRTPRPVRVITKAPIIRLETASPPTRIRTTTSGVPRGGEPNQRPELK	498
human	*****VS*****	
mouse	NHIDRDVAWVGTYFEVKIPSDTFYDNEDTTDDKLLKLTILKREQLVGEKS	548
human	*****H*****	
mouse	WVQFNNSQLMYGLPDSHVGKHEYFMHATDKGGLSAVDAFEIHVHKRPQ	598
human	*****R***	
		†
mouse	GDKAPARFKARLAGDPAPVNDIHKKIALVKKLAFAFGDRNCSSITLQNI	648
human	**R*****K*FV***L*L*****T*****	
		†
mouse	TRGSIVVEWNTNLTLPLEPCPKQI IGLSRR IADENKPRPAFNSNALEPDF	698
human	*****A*****EDD*****	
mouse	KALSIAVTGGSGCRHLQFIPVAPPSPGSSAAPATEVPRDRPEKSSSEDDVY	748
human	**T**T*****V**RRVP*E**P*****	
mouse	LHTVI PAVVVAAILLIAGI IAMI CYRKKRKGKLTLEDQATFIKKGVPIIF	798
human	*****I*****	
mouse	ADELDDSKPPSSSMLIILQEEKAPLPPPEY PNQSMPE TPLNQDTVGEY	848
human	*****V*****M**	
mouse	TPLRDEDPNAPPYQPPPPFTAPMEGKGRKNTPEYRSPPEYVPP-	893
human	*****V*****-	

**Figure 1.** Complete amino acid sequence of *Dag1*. A comparison of the predicted amino acid sequences of mouse (this study) and human (3) dystroglycan is shown. (\*): Indicates a human residue identical to the corresponding mouse residue. Bold underline indicates the signal peptide sequence. Boxed amino acids are the transmembrane domains. Shaded amino acids are the dystrophin binding site. (-): Indicates the stop codons. (†): Is above amino acids that are predicted to be N-linked glycosylation sites. Only those sites that are conserved among all known dystroglycan sequences are indicated. (‡): Is above amino acids that are potential glycosaminoglycan chain addition sites.

and then matured *in vitro* after thawing. Animals arising from these embryos were test bred to C57 BL/6J mice. A male exhibiting a high degree of coat color chimerism transmitted the ES cell genome to 100% of its offspring. Animals heterozygous for *Dag1<sup>neo2</sup>* appear healthy and breed normally. Interestingly, Northern blot analysis of skeletal muscle RNA showed that dystroglycan transcript levels in the heterozygotes were only 10–20% lower than those in wild-type mice, suggesting a compensatory increase in the steady state expression level of mRNA derived from the untargeted allele (Fig. 3D). Correspondingly, dystroglycan protein levels in skeletal muscle were also comparable between wild-type and heterozygous *Dag1<sup>neo2</sup>* mice (data not shown). In contrast, we did not detect dystroglycan mRNA in homozygous *Dag1<sup>neo2</sup>* embryos (data not shown) or dystroglycan immunoreactivity in mutant embryos

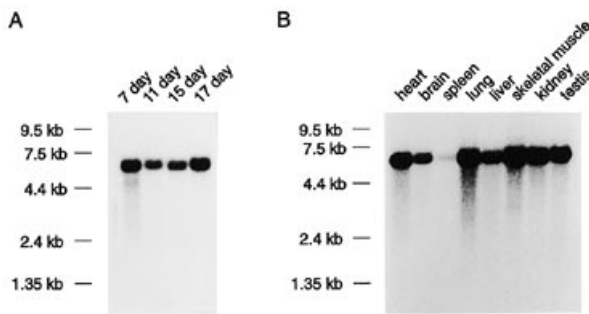


**Figure 2.** Developmental and tissue-specific expression of *Dag1*. Northern blot analysis of dystroglycan mRNA expression in whole mouse embryos collected between E7 and E17 (A) and in selected adult mouse tissues (B). A single 5.8 kb dystroglycan mRNA is apparent at each developmental stage and in each tissue analyzed.

using antibodies directed toward the C-terminus of  $\beta$ -dystroglycan (see below) indicating that *Dag1<sup>neo2</sup>* is a true null allele of *Dag1*. For simplicity, we will hereafter refer to homozygous *Dag1<sup>neo2</sup>* embryos as *Dag1*-null embryos.

The genotypes of surviving offspring from 14 heterozygote intercrosses were either wild-type or heterozygous for *Dag1<sup>neo2</sup>* in an ~1:2 ratio (20:42). No *Dag1*-null pups have been born. These data suggested Mendelian inheritance of a recessive embryonic lethal trait. To investigate this further, we dissected embryos derived from heterozygote intercrosses between embryonic day (E)7.5 and E10.5 and genotyped them using a PCR-based assay (Fig. 3C). We found a tight correlation between the *Dag1*-null genotype and an abnormal embryonic morphology (Table 1).

**Table 1.** Genotypes of offspring from heterozygote intercrosses

Age	Number of embryos	Genotype		
		+/+	+/-	-/-
E7.5	20	3	12	5
E8.5	27	4	15	8
E9.5	40	10	23	7
E10.5	33	7	15	11
Total	120	24	65	31

Embryos were dissected from uteri between E7.5 and E10.5, scored for morphology, and genotyped by PCR analysis (see Fig. 3C). All morphologically normal embryos were either homozygous wild-type (+/+) or heterozygous for the *Dag1<sup>neo2</sup>* allele (+/-), whereas all morphologically abnormal embryos were homozygous for *Dag1<sup>neo2</sup>* (-/-). The genotypes show an approximate 1 (+/+):2 (+/-):1 (-/-) ratio. From E7.5 to E10.5, the (-/-) embryos became progressively more disorganized and resorbed. TBASE accession nos: (+/-), TG-000-04-258 and (-/-) TG-000-04-259.

The gross morphology of mutant embryos began to diverge significantly from that of phenotypically normal littermates at E6.5. By E7.5, dramatic differences were apparent between the normal (wild-type and heterozygous) and abnormal *Dag1*-null embryos (Fig. 4A and B). In particular, the abnormal embryos were much smaller than normal littermates and lacked a well defined embryonic region. By E10.5 most abnormal embryos were substantially resorbed, and only a small mass of embryonic tissue was apparent (data not shown).

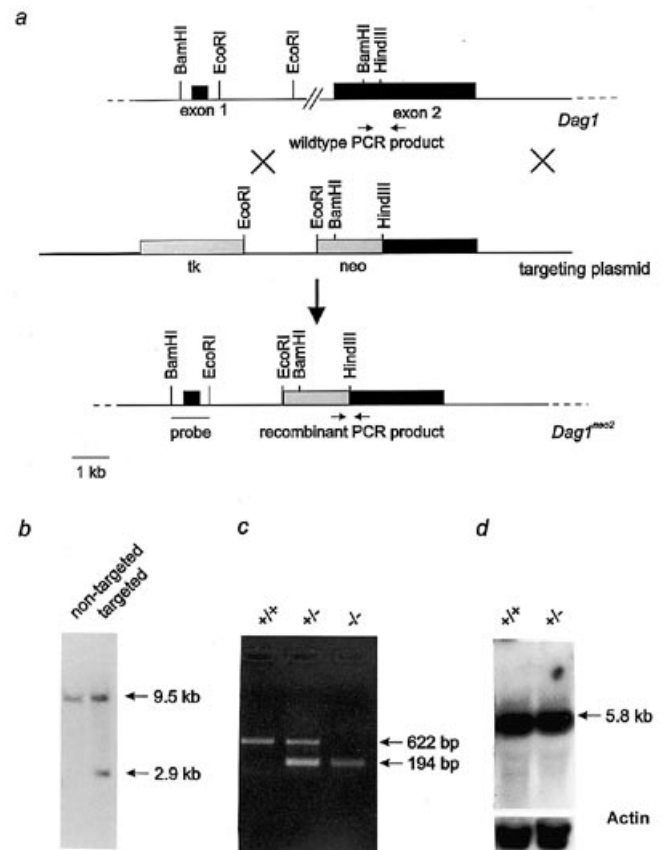


**Figure 3.** Disruption of *Dag1*. The targeting strategy is depicted in (a). Schematic shows the wild-type locus (top) with pertinent restriction sites indicated. The black boxes represent the two exons present in *Dag1*. The targeting plasmid (middle) was designed to replace a portion of exon 2 with the *neo* gene following homologous recombination (denoted by Xs), producing *Dag1<sup>neo2</sup>* (bottom). *Dag1<sup>neo2</sup>* bears a deletion in exon 2 including the splice acceptor site and a significant portion of the coding sequence present in  $\alpha$ -dystroglycan. Southern analysis of ES cell clones (b). Insertion of the *neo* gene into exon 2 yields a new 2.9 kb *Bam*HI fragment which hybridizes with exon 1 probe in addition to the 9.5 kb wild-type fragment. Shown are the results from a non-targeted clone (left) and a targeted clone (right). PCR analysis (c) of E9.5 embryos. *Dag1* generates a PCR product of 622 bp and *Dag1<sup>neo2</sup>* one of 194 bp. Shown are the results for homozygous wild-type (+/+), heterozygous (+/-), and homozygous *Dag1<sup>neo2</sup>* (-/-) embryos. Northern analysis (d) of dystroglycan mRNA expression in adult mice. The transcript levels are similar in (+/+) and (+/-) mice. Furthermore, using a cDNA probe for the entire dystroglycan coding sequence, we only detect the 5.8 kb *Dag1* transcript, indicating that a potential mutant transcript from *Dag1<sup>neo2</sup>* in the (+/-) mice is either non-existent, or below the limit of detection of this assay.

To examine the mutant phenotype in more detail, we performed histological analysis. All early post-implantation embryos derived from heterozygote intercrosses were indistinguishable from one another at E4.5 (data not shown). The histology of early egg cylinder stage embryos (E5.5) was comparable, except that in about one quarter of those examined (4/15) we noted the presence of maternal red blood cells in the yolk sac cavity (Fig. 4D). These red blood cells had presumably entered the yolk sac cavity from the subjacent maternal sinusoids that begin to develop around E5.5. In advanced egg cylinder stage (E6.5) embryos, approximately one quarter of those examined (9/32) were clearly histologically abnormal. Compared to normal embryos (Fig. 4E),

these presumptive *Dag1*-null embryos (Fig. 4F) typically possessed a much smaller embryonic region and lacked any significant development of the extraembryonic ectoderm. Again, in these abnormal E6.5 embryos, we observed maternal red blood cells in the yolk sac cavity. We noted that endodermal differentiation had taken place in the mutant embryos, as visceral endoderm was clearly evident, and in some sections we could also see parietal endoderm cells. Also, the abnormal embryos displayed a well-formed pro-amniotic cavity. In primitive streak stage embryos at E7.5, abnormal embryos lacked any recognizable mesodermal tissue (data not shown). Preliminary experiments showed that there was no *Brachyury* expression in the mutant embryos at E7.5 and E8.5, further indicating that the mutant embryos fail to gastrulate and do not form mesoderm (data not shown). We confirmed that these abnormal embryos were indeed *Dag1*-null embryos by immunostaining (see Fig. 5). On the whole, these data indicate that the *Dag1*-null embryos fail to progress beyond the early egg cylinder stage of development.

In an attempt to determine the earliest stage at which the developmental program of the *Dag1*-null embryos begins to diverge from control littermates, we examined the growth of blastocysts derived from heterozygote intercrosses *in vitro*. The size and cellular composition of these blastocyst cultures was comparable between those expressing dystroglycan and those not expressing dystroglycan (data not shown), indicating that pre-implantation development occurs normally in the absence of dystroglycan. At least some aspects of implantation had occurred in the mutant embryos; they seemed to elicit a normal decidual response (see Fig. 5D) and invasive trophoblast giant cells were evident by both histological and immunohistochemical analysis (see Fig. 7D). Together, these data suggest that the phenotype in *Dag1* null embryos is manifest after implantation.

#### Localization of dystroglycan protein in egg cylinder stage embryos

In part because dystroglycan had not previously been thought to have a developmentally important role, data on its expression in the early embryo is lacking. An earlier study showed that dystroglycan mRNA is present throughout the embryo at E9.5 (18). We determined that dystroglycan mRNA is abundantly expressed at E7.0 (Fig. 2A) and afterward, but not in ES cells (data not shown). We examined the localization of dystroglycan protein in normal egg cylinder embryos by immunostaining with a specific anti-dystroglycan antibody (Fig. 5). Dystroglycan staining is also evident outlining maternal decidual cells (Fig. 5A and D). During the preparation of this manuscript, it was reported that dystroglycan mRNA is upregulated in the deciduum at the peri-implantational stage (19). In normal E6.5 embryos (Fig. 5A–C), there is intense dystroglycan labeling apposed to two embryo-derived basement membrane structures—Reichert's membrane and the basement membrane separating the visceral

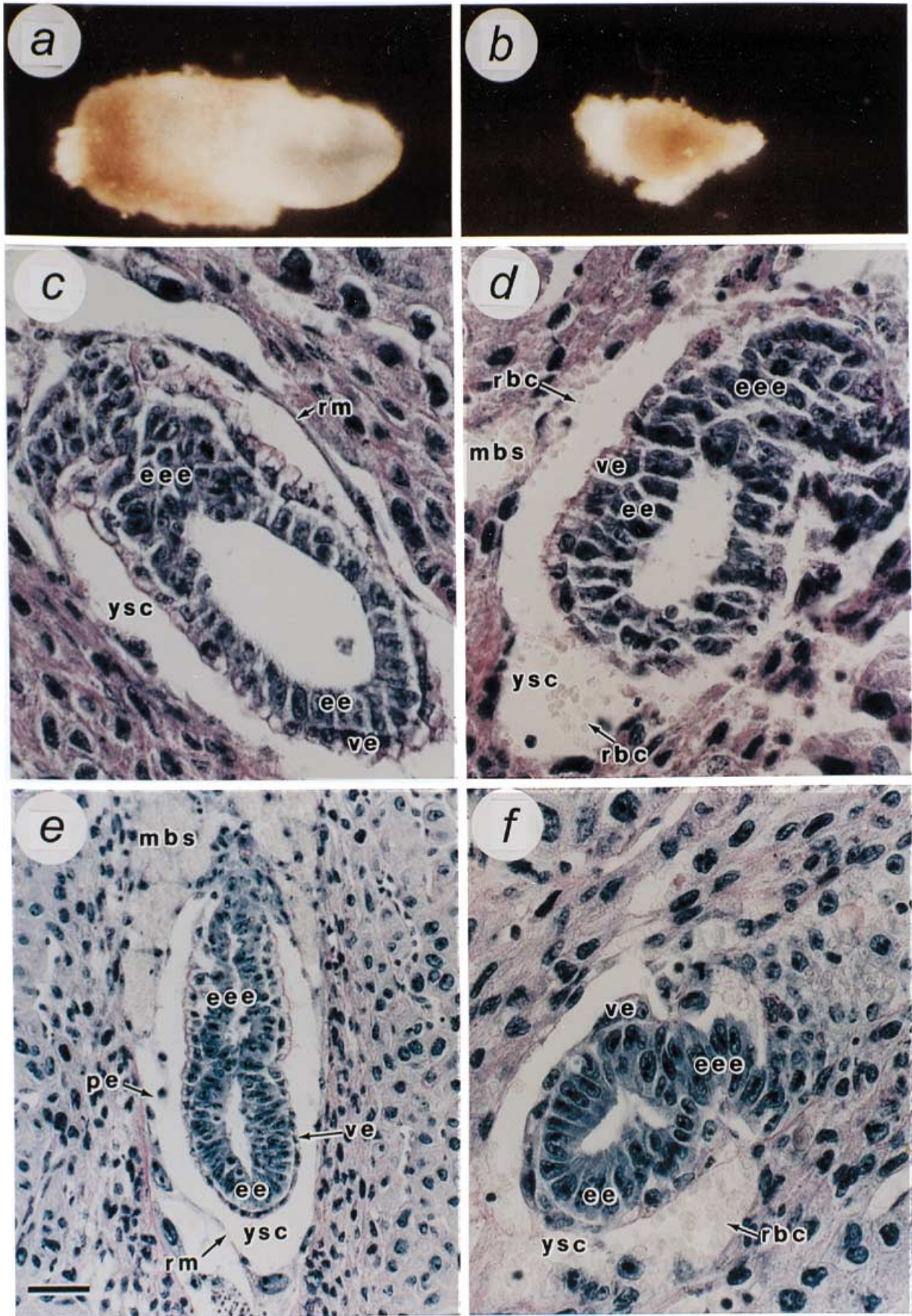
endoderm and ectoderm. With respect to the Reichert's membrane localization, we have not yet determined whether one or both cell types associated with that structure, i.e. trophoblast and parietal endoderm, express dystroglycan on their surfaces. However, as dystroglycan staining appears continuous throughout Reichert's membrane and neither the trophoblast nor parietal endoderm are continuous cell layers, there is the suggestion that dystroglycan is expressed on both cell types. Dystroglycan localization in apposition to these embryonic basement membranes is consistent with its localization pattern in adult tissues. There is also somewhat less pronounced pericellular labeling of most, if not all, other embryonic cells. Similar staining patterns were observed in E5.5 embryos (data not shown). Specificity of these staining patterns is demonstrated by their absence in mutant embryos (Fig. 5D–F). However, as would be predicted, dystroglycan staining is still present on the maternal decidual cells from uterine sections bearing *Dag1*-null embryos (Fig. 5D).

#### Disruption of Reichert's membrane structural proteins in *Dag1*-null embryos

The histological analysis indicated that the presence of maternal red blood cells in the yolk sac cavity was an early step in the failure of the developmental program of *Dag1*-null embryos. Since Reichert's membrane forms the only continuous barrier between the embryonic yolk sac cavity and the maternal blood present in the subjacent sinuses, the mutant phenotype suggests impaired function of this structure. This finding, coupled with the localization of dystroglycan apposed to Reichert's membrane in the egg cylinder stage embryos, supports the notion that dystroglycan is required for the appropriate development of Reichert's membrane. To probe this idea further, we examined the distribution of laminin and collagen IV, two principal structural components of Reichert's membrane (20). Indeed, the localization of both of these extracellular matrix proteins is perturbed in the *Dag1*-null embryos. Instead of the continuous labeling of laminin and collagen IV seen in Reichert's membrane of normal embryos (Fig. 6B and C), there were only occasional 'patches' of laminin and collagen IV staining in the location where Reichert's membrane should be found in the mutant embryos (Fig. 6E and F). In contrast, laminin and collagen IV staining in the basement membrane between the visceral endoderm and ectoderm in *Dag1*-null embryos is apparently normal. In essence, the *Dag1*-null embryos lack a continuous Reichert's membrane which most probably accounts for the presence of maternal red blood cells in the yolk sac cavity.

Since disruption of Reichert's membrane in the *Dag1*-null embryos could be a secondary consequence of the lack of parietal endoderm cells, which synthesize the extracellular matrix components of that structure, it was important to assay for the presence of these cells. Because the overall pattern of laminin and collagen IV staining was so profoundly disrupted in the

**Figure 4.** Gross morphology and histology of normal and abnormal embryos. Morphology of (A) normal (+/+) and (B) abnormal (-/-) littermates at E7.5. The genotypes of these embryos were confirmed by PCR analysis. The reduced size of the embryonic region was characteristic of the abnormal embryos. Sagittal sections of PAS-stained (C and E) normal and (D and F) presumptive *Dag1<sup>neo2</sup>* homozygous mutant embryos. Normal E5.5 embryo (C) with tissue layers delineated. Its littermate (D) looks normal, except for the presence of maternal red blood cells in the yolk sac cavity. At E6.5 abnormal embryos (F) are much smaller compared to normal (E) littermates. Again, maternal red blood cells were present in the yolk sac cavity of the abnormal E6.5 embryos. Abbreviations: ee, embryonic ectoderm; eee, extra-embryonic ectoderm; mbs, maternal blood sinus; pe, parietal endoderm; rbc, maternal red blood cells; Rm, Reichert's membrane; ve, visceral endoderm; ysc, yolk sac cavity. Scale bars: C, D and F, 25  $\mu$ m; E, 50  $\mu$ m.



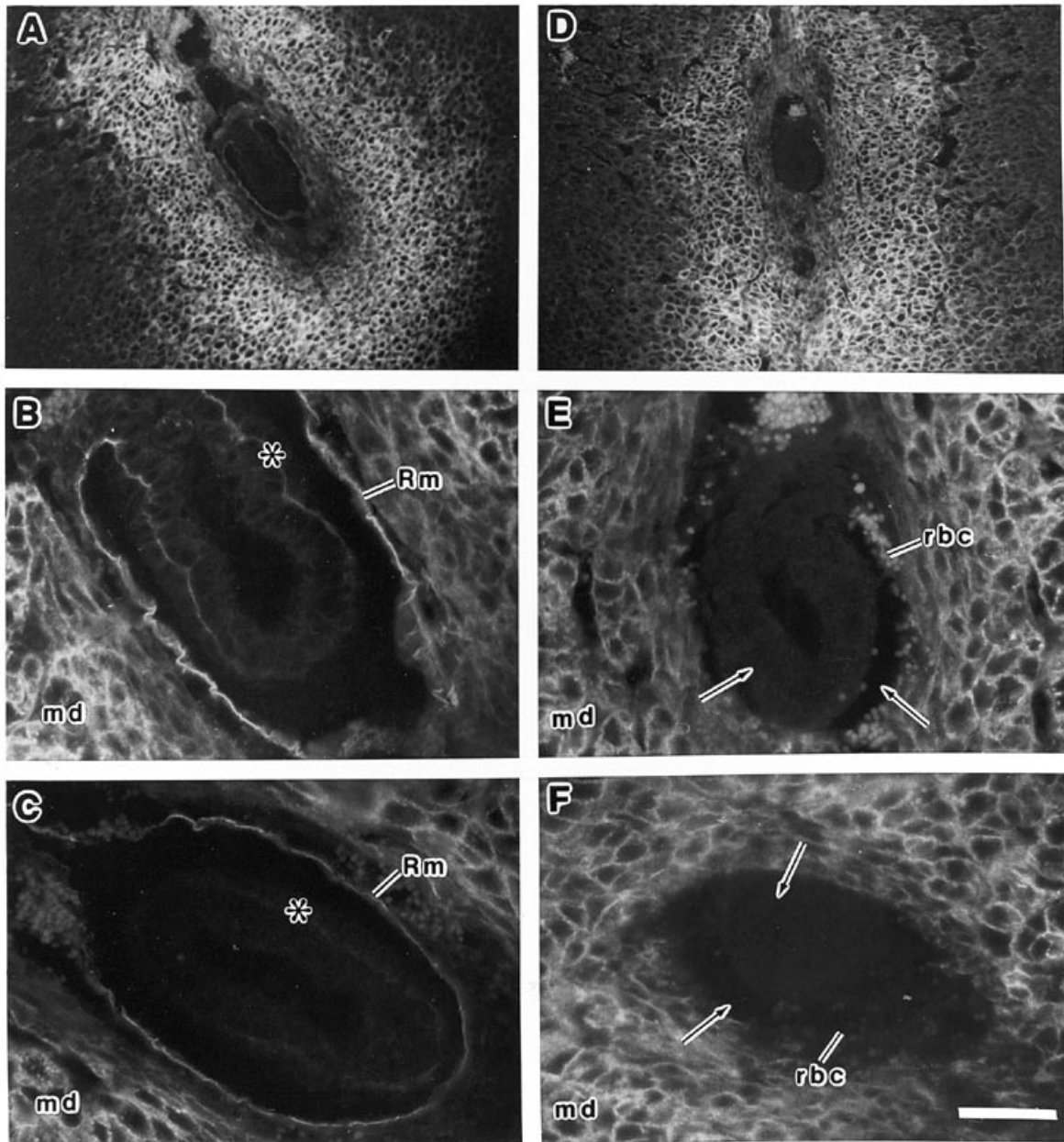


**Figure 5.** Localization of dystroglycan protein in egg cylinder stage embryos. Sections taken from E6.5 normal (A, B and C) and abnormal (D, E and F) littermates were processed for immunofluorescence with a specific anti-dystroglycan antibody as described in Materials and Methods. (A and D) Low magnification images of the uterine section showing dystroglycan staining in the maternal decidual cells. The edge of the uterine section extends beyond the edge of the field shown on all sides. (B) Higher magnification of (A), and (C), another embryo, show the detailed dystroglycan staining in the normal embryos and associated extraembryonic membranes. Dystroglycan staining is prominently localized in apposition to Reichert's membrane (Rm) and the basement membrane between the visceral endoderm and ectoderm (\*). There is fainter staining surrounding most of the other cells in the embryo. Also, staining in the maternal decidual cells (md) can be seen in these higher magnification images. (E) Higher magnification of (D), and (F), another embryo, show dystroglycan staining of typical abnormal embryos. Autofluorescent maternal red blood cells (rbc) can be seen in the yolk sac cavity. There is a complete absence of dystroglycan staining in these embryos, demonstrating that these are *Dag1*-null embryos. The approximate positions where prominent dystroglycan staining should be are indicated by arrows. Scale bars: A and D, 200 $\mu$ m; B, C, E and F, 50  $\mu$ m.

*Dag1*-null embryos, it was difficult to use these molecules as reliable markers for parietal endoderm cells. Instead, we used an antibody specific for the Pem homeodomain protein which is expressed in a variety of extraembryonic lineages, including parietal endoderm cells, around E5.5 (21). Figure 7 shows double-label immunofluorescence staining of laminin (Fig. 7A, D and G), Pem (Fig. 7B, E and H) and nuclear counterstaining

(Fig. 7C, F and I) in control littermate (Fig. 7A–C) and *Dag1*-null E5.5 embryos (Fig. 7D–I). As expected, the anti-Pem antibody stains the nuclei of a variety of extraembryonic cell types including parietal endoderm cells. That these cells (arrows in Fig. 7) are indeed parietal endoderm cells, and not the juxtaposed trophoblast cells, which also react positively with the anti-Pem sera, is supported by both their co-labeling with anti-laminin

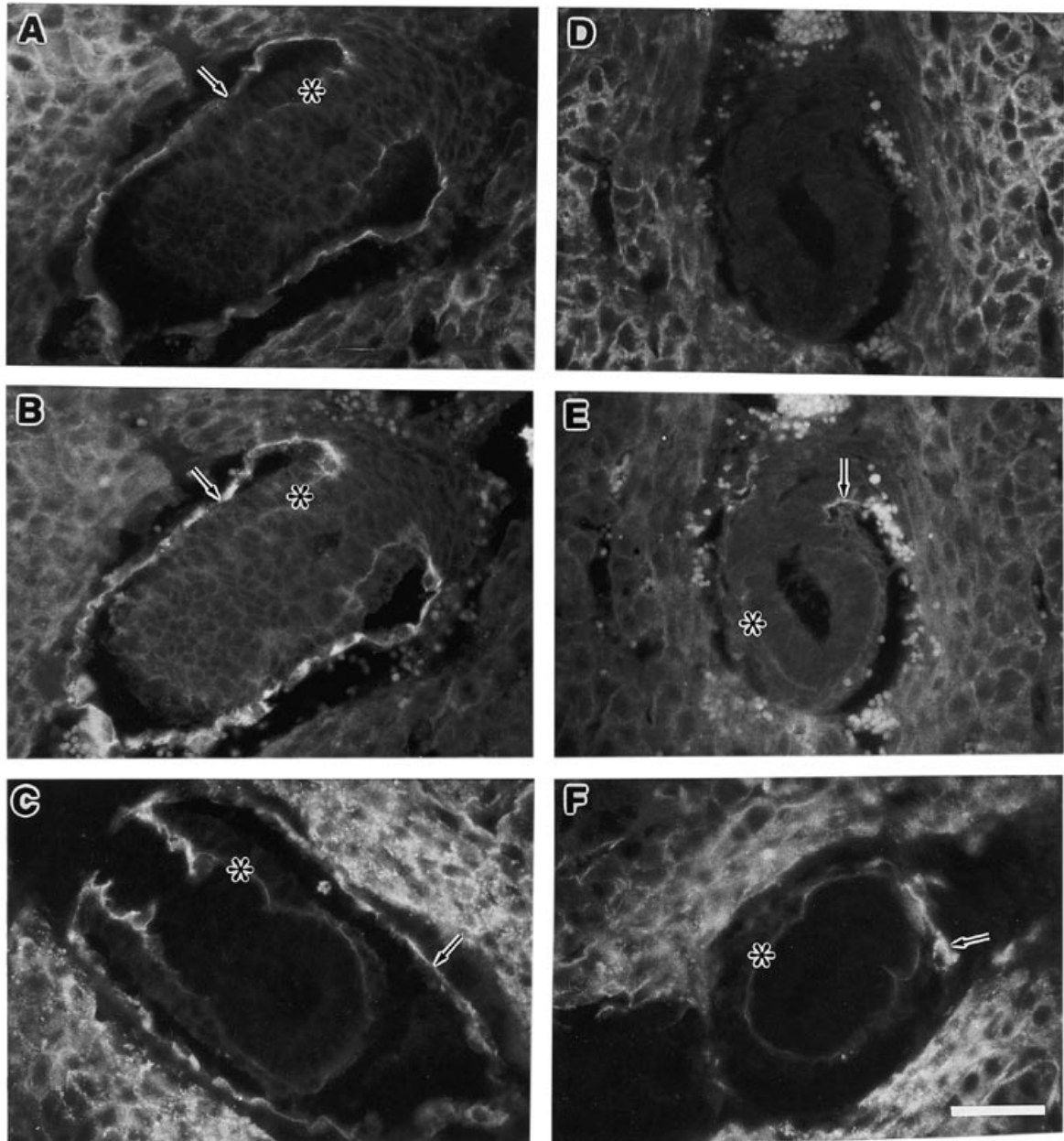


**Figure 6.** Analysis of Reichert's membrane structural proteins in *Dag1*-null embryos. Immunofluorescence analysis of dystroglycan (**A** and **D**), laminin (**B** and **E**) and collagen IV (**C** and **F**) expression in a control littermate (**A–C**) and a *Dag1* null (**D–F**) embryo. E6.5 littermates were stained with the appropriate antibodies as described in Materials and Methods. (**A** and **B**) and (**D** and **E**) are paired images from embryos simultaneously stained for dystroglycan and laminin. (**C** and **F**) Adjacent sections to the ones shown in (**A** and **B**) and (**D** and **E**), respectively. Note that the embryo shown in (**D–F**) is the same one shown in Figure 5D and E. In normal embryos, dystroglycan is colocalized with laminin and collagen IV in Reichert's membrane (arrows) and in the basement membrane between the visceral endoderm and ectoderm (\*). However in the *Dag1* null embryos, the normally continuous Reichert's membrane staining is reduced to 'patches' (arrows), but the staining between the visceral endoderm and ectoderm (\*) is still present in these mutants. Scale bar: A–F, 50  $\mu$ m.

antibodies and their anatomical position adjoined to the embryo-proximal face of Reichert's membrane. In the *Dag1*-null embryos, Pem-positive parietal endoderm cells can be seen throughout the lining of the yolk sac cavity, although the laminin staining for Reichert's membrane is discontinuous. These parietal endoderm cells also stain with the anti-laminin antibody, explaining the 'patchy' laminin and collagen IV staining noted above. This result demonstrates that parietal endoderm cells differentiate and migrate appropriately in *Dag1*-null embryos,

indicating that the Reichert's membrane defects in these embryos are not due to a lack of parietal endoderm.

We also note that the overall staining pattern for Pem in *Dag1*-null embryos is comparable to that of control littermates. In particular, Pem-positive trophoblast giant cells have clearly invaded the surrounding uterine stroma (arrowheads in Fig. 7). These results further support the notion that early differentiation of extraembryonic lineages and implantation occur normally in *Dag1*-null embryos.

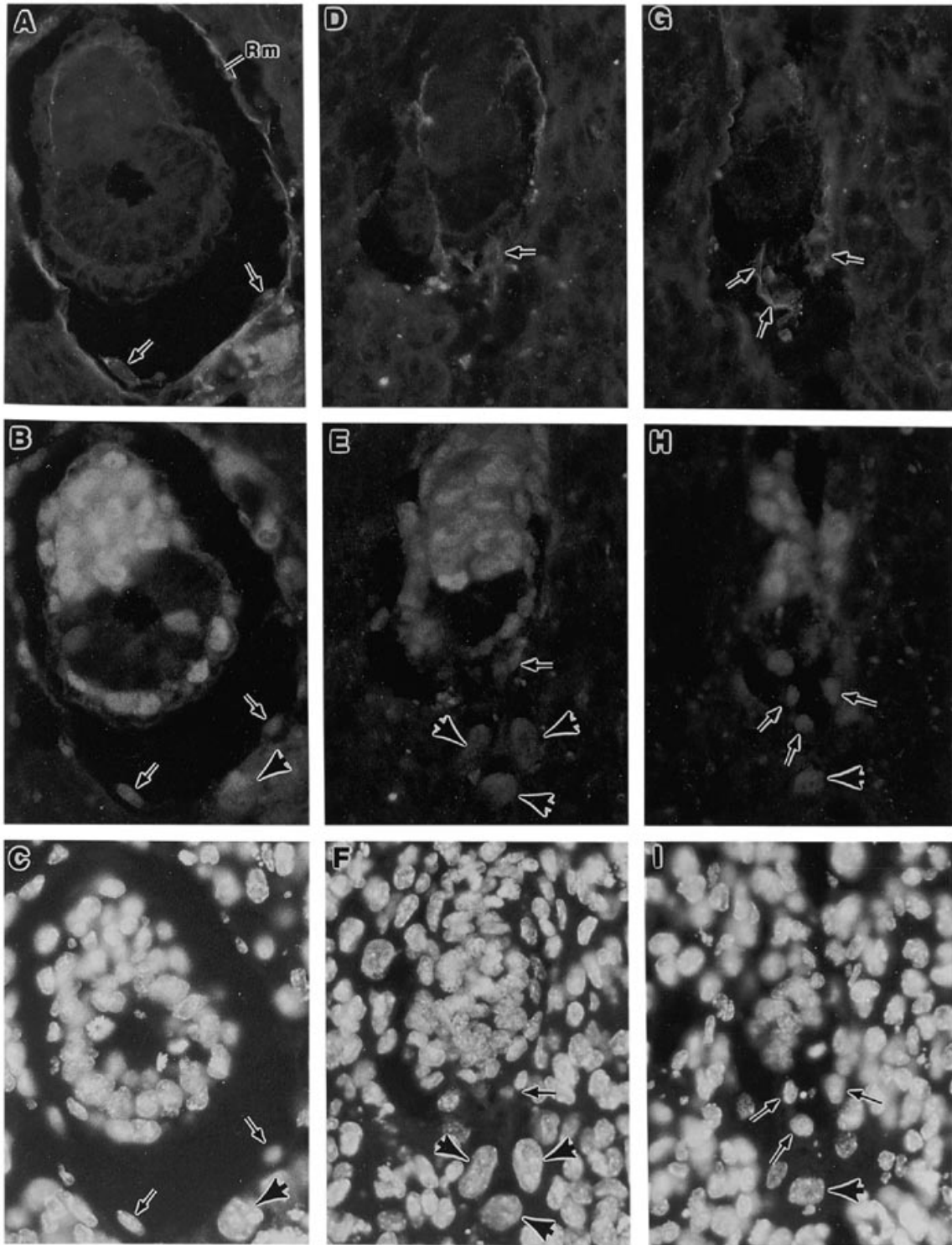


**Figure 7.** Parietal endoderm cells are present in *Dag1*-null embryos. Double-label immunofluorescence analysis of laminin (A, D and G), Pem (B, E and H) and nuclear counterstaining (C, F and I) in a control littermate (A–C) and two different sections from a *Dag1*-null embryo (D–I). E5.5 littermates from heterozygous intercrosses were sectioned, and the status of dystroglycan expression in the embryos was determined by staining with an anti-dystroglycan antibody. Separate sagittal sections were simultaneously stained for laminin and Pem and nuclei were counterstained with 4',6-diamidino-2-phenylindole. Pem marks the nuclei of a variety of extraembryonic cells, including parietal endoderm cells (arrows) which co-label with laminin. Parietal endoderm cells are clearly present in the *Dag1*-null embryo. The section shown in (D–F) is a comparable plane to (A–C) and is through the center of the embryo. (G–I) A more tangential section from the same embryo in (D–F). Arrowheads denote trophoblast giant cells. Rm, Reichert's membrane.

## DISCUSSION

Our results indicate that dystroglycan is required for normal murine embryonic development beyond the egg cylinder stage. The mutant phenotype suggests that the developmental program of *Dagl*-null embryos fails as a result of a disruption of Reichert's membrane. This was first indicated by the conspicuous presence of maternal red blood cells in the yolk sac cavities of E5.5 *Dagl*-null embryos, which otherwise appear histologically normal. We have also shown that two of the major structural components of Reichert's membrane, laminin and collagen IV, are specifically disrupted in *Dagl*-null embryos, despite the fact that the parietal endoderm cells which secrete these molecules are present in those embryos. Together, these results demonstrate that *Dagl*-null embryos lack a structurally and functionally definable Reichert's membrane, indicating that dystroglycan is necessary for the proper development of that structure. Disruption of the barrier function of Reichert's membrane could lead to lethality due to a toxic effect of direct exposure of the embryo to the maternal circulation or uterine environment. Alternatively, Reichert's membrane is purported to play a role in materno-embryonic exchange (22,23), and therefore its disruption may lead to wasting and ultimately death of the *Dagl*-null embryos.

The localization of dystroglycan protein in the egg cylinder stage embryo is consistent with a role for dystroglycan in the development of Reichert's membrane. However, dystroglycan is also expressed throughout the embryo, most notably in apposition to the basement membrane between the visceral endoderm and ectoderm. In principle, a lack of dystroglycan function in this structure could lead to the death of the *Dagl*-null embryo. However, at least one developmental event, pro-amniotic cavity formation, that is thought to depend on this basement membrane (24) seems to occur normally in *Dagl*-null embryos.

How might dystroglycan be involved in the development of Reichert's membrane? Reichert's membrane is formed between the trophoblast and parietal endoderm beginning shortly after implantation. Parietal endoderm cells differentiate from the hypoblast, migrate along the mural trophoctoderm of the blastocoel cavity, the prospective yolk sac cavity, and synthesize copious amounts of laminin and collagen IV which are incorporated into Reichert's membrane (25,26). Dystroglycan does not appear to be required for the differentiation or migration of parietal endoderm cells. Indeed, we show that parietal endoderm cells in the *Dagl*-null embryos express at least three markers of differentiated parietal endoderm—laminin, collagen IV, and Pem—and that they can achieve their proper localization on the inner face of the yolk sac cavity. It is also unlikely that a lack of dystroglycan has an effect on the biosynthesis of the extracellular matrix proteins that comprise Reichert's membrane because laminin and collagen IV are expressed by parietal endoderm cells in 'patches' and in the basement membrane between the visceral endoderm and ectoderm.

Dystroglycan's known role as a laminin receptor in adult tissues and its tight co-localization with laminin in the embryo suggest other possibilities for its involvement in the development of Reichert's membrane. For instance, dystroglycan may bind to laminin and thereby mediate the organization of the extracellular matrix constituents of Reichert's membrane. This might be accomplished by simply anchoring laminin to the surface of the

cellular components of the parietal yolk sac. Perhaps more intriguingly, dystroglycan may catalyze the assembly of laminin networks. Interestingly, Kadoya *et al.* (27) found that antibodies against the E3 domain of laminin-1, the same portion of laminin to which  $\alpha$ -dystroglycan binds, perturb basement membrane formation in an embryonic submandibular gland culture system. There is as yet no known direct connection between dystroglycan and collagen IV, but laminin and collagen IV are molecularly linked by entactin/nidogen (28) and recent studies suggest that collagen IV network assembly may depend on laminin network assembly (29). If dystroglycan is required for the anchorage or assembly of laminin networks, and therefore indirectly for the assembly of collagen IV networks, then in *Dagl*-null embryos, laminin and collagen IV synthesized by parietal endoderm cells might diffuse away into the maternal circulation instead of forming the insoluble Reichert's membrane matrix. Perhaps continuous laminin and collagen IV staining persists in the basement membrane between the visceral endoderm and ectoderm in *Dagl*-null embryos because these molecules are trapped between two continuous epithelial cell layers. Such a role for dystroglycan in the organization of extracellular matrix proteins might explain its previously demonstrated involvement in other systems such as the developing neuromuscular junction and kidney, where there is, in each case, ongoing synthesis and assembly of extracellular matrix proteins into basement membrane structures.

Reichert's membrane is a particular feature of the rodent embryo. However, if dystroglycan is generally involved in the development of basement membranes, it would certainly seem to be a requisite for normal human development. Our findings strongly indicate that the failure to identify null mutations in *DAG1* linked to muscular dystrophies in humans is due to early embryonic lethality of such mutations, although they do not rule out the possibility that more subtle mutations in dystroglycan could play a role in human disease. Despite the fact that there may be no primary genetic defects in dystroglycan associated with skeletal muscle pathology, a partial loss of dystroglycan function may be an underlying feature of Duchenne and limb-girdle muscular dystrophies. In Duchenne muscular dystrophy patients and *mdx* mice, there is a drastic reduction of dystroglycan protein in the sarcolemma (1,30), where it would normally be interacting with laminin-2 in the muscle cell basement membrane. And in the cardiomyopathic hamster, a candidate animal model for limb-girdle muscular dystrophy, the association of  $\alpha$ -dystroglycan with the sarcolemma is disrupted (31). Therefore, while the prevailing notion is that dystroglycan serves as a sort of transmembrane mechanical linkage, in light of our present results, it seems reasonable to propose that the reduction or perturbation of dystroglycan in the sarcolemma might also lead to extracellular defects in the organization of the muscle cell basement membrane. In other skeletal muscle diseases, there is clear involvement of the extracellular matrix. Certain forms of congenital muscular dystrophy and Bethlem myopathy are caused by mutations in the  $\alpha 2$ -chain laminin-2 and the  $\alpha 1$  and  $\alpha 2$  chains of type VI collagen, respectively (32,33). It is interesting to speculate that the molecular mechanisms that lead to pathological cell death in each of the aforementioned muscle diseases and to the demise of *Dagl*-null embryos might be related.

## MATERIALS AND METHODS

### Isolation and expression of *Dag1*

*Dag1* was isolated from a  $\lambda$  FIXII 129/Sv genomic library by homology screening using a radiolabeled human cDNA (3). The *Dag1* sequence has been submitted to GenBank (accession number U48854). For Northern blot analysis we probed commercially prepared (Clontech) blots of developing mouse embryos and adult mouse tissues containing 2  $\mu$ g polyA(+) RNA with a radiolabelled full-length rabbit dystroglycan cDNA (2) probe. Hybridization was carried out using standard methods. Blots were exposed for autoradiography.

### Generation of *Dag1*-null mice

From the *Dag1* sequence, we cloned regions of dystroglycan homology flanking the *neo* gene into the positive-negative selection vector pPNT. A 5 kb *NotI*-*HindIII* fragment carrying the 3' portion of exon 2 was subcloned into a pBluescript vector, isolated as a *NotI*-*XhoI* fragment, and inserted into *NotI*-*XhoI* cut pPNT. The resulting plasmid was cut with *EcoRI* and a 1.9 kb *EcoRI* fragment of intronic sequence was inserted into this site. Following linearization at a unique *NotI* site, 25  $\mu$ g of targeting plasmid was electroporated (240 V, 500  $\mu$ F; Bio-Rad Gene Pulser) into  $2 \times 10^7$  dispersed R<sub>1</sub> ES cells (34). The ES cells were maintained on feeder layers. Southern analysis for detection of targeted ES cells was performed according to standard methods. PCR was carried out for genotyping embryos and weanling mice. For detection of *Dag1*, we used the following primer pairs: forward (5'-TACCACAACCTCGGAGGCCATCCA-3'); reverse (5'-TGA-TGTTCTGCAGGGTGCACGGAG-3'). For detection of *Dag1<sup>neo2</sup>*, we used the following primer pairs: forward (5'-CAGGC-AGGCCATACATGA-3'); reverse (5'-AGAGCCCACTTGTG-TAGCG-3'). Northern blot analysis was carried out as described above on 20  $\mu$ g total RNA isolated from skeletal muscle dissected from wild-type and heterozygous *Dag1<sup>neo2</sup>* littermates. Band intensity on autoradiographs was quantitated by densitometry.

### Histology and immunohistochemistry

For histological analysis, the decidual sacs from timed matings were dissected, fixed in Pen-Fix (Richard Allen Inc.) and embedded in paraffin. We defined the morning that the vaginal plug was observed as E0.5. Sections (7  $\mu$ m) were stained using periodic acid-Schiff histochemistry. For immunostaining, embryos were fixed in either Pen-Fix or 4% paraformaldehyde and embedded in paraffin. Seven micron thick sections were deparaffinized with xylenes, hydrated in a graded series of ethanol and blocked with PBS + 1% BSA. Primary antibodies, anti- $\beta$ -dystroglycan affinity purified against the 15 C-terminal amino acids of dystroglycan (35) anti-human placental laminin (36), anti-collagen  $\alpha$ 1/2 (IV) (Southern Biotechnology Associates, Catalog no. 1340-01), and anti-Pem (21) were diluted 1:10, 1:500, 1:100, and 1:5000, respectively, in PBS + 1% BSA and reacted overnight with sections. Secondary antibodies, conjugated to indocarbocyanine-3 or fluorescein isothiocyanate, were purchased from Jackson Immuno Research Labs and used according to the manufacturer's directions. In some experiments, nuclei were counterstained with 4',6-diamidino-2-phenylindole (Sigma)

## ACKNOWLEDGEMENTS

We thank Deanna Hunt for technical support. We acknowledge the generous gifts of the R<sub>1</sub> ES cells from Andras Nagy (Samuel Lunenfeld Research Institute, Toronto), the pPNT plasmid from Richard Mulligan (Whitehead Institute, Cambridge), the anti-laminin antisera from Paul Durham and Jeanne Snyder (University of Iowa, Iowa City), the anti-Pem antisera from Carol MacLeod (University of California at San Diego, La Jolla), and consultation on the histology from James Cross (Mount Sinai Hospital, Toronto) and Brigid Hogan (Vanderbilt University Medical School, Nashville). RAW is grateful to Oliver Smithies, Nobuyo Maeda and Beverly Koller for help in establishing a gene targeting laboratory. RAW and KPC are supported by grants from the Muscular Dystrophy Association, MDH is supported in part by a fellowship from the University of Iowa Cardiovascular Center, KJD is partially supported by grants from NIH NIDR and NIH RO1 DE09170 to Dr Andrew Russo, and KPC is an Investigator of the Howard Hughes Medical Institute.

## ABBREVIATIONS

DGC, dystrophin-glycoprotein complex; E, embryonic day; ES, embryonic stem; PCR, polymerase chain reaction.

## REFERENCES

1. Ervasti, J.M., Ohlendeick, K., Kahl, S.D., Gaver, M.G. and Campbell, K.P. (1990) Deficiency of a glycoprotein component of the dystrophin complex in dystrophic muscle. *Nature*, **345**, 315-319.
2. Ibraghimov-Beskrovnyaya, O., Ervasti, J.M., Leveille, C.J., Slaughter, C.A., Sernett, S.W. and Campbell, K.P. (1992) Primary structure of dystrophin-associated glycoproteins linking dystrophin to the extracellular matrix. *Nature*, **355**, 696-702.
3. Ibraghimov-Beskrovnyaya, O., Milatovich, A., Ozcelik, T., Yang, B., Koepnik, K., Franke, U. and Campbell, K.P. (1993) Human dystroglycan: skeletal muscle cDNA, genomic structure, origin of tissue specific isoforms and chromosomal localization. *Hum. Mol. Genet.*, **2**, 1651-1657.
4. Sunada, Y., Bernier, S.M., Kozak, C.A., Yamada, Y. and Campbell, K.P. (1994) Deficiency of merosin in dystrophic *dy* mice and genetic linkage of laminin M chain gene to *dy* locus. *J. Biol. Chem.*, **269**, 13729-13732.
5. Yoshida, M., Suzuki, A., Yammamoto, H., Noguchi, S., Mizuno, Y. and Ozawa, E. (1994) Dissociation of the complex of dystrophin and its associated proteins into several unique groups by *n*-octyl- $\beta$ -D-glucoside. *Eur. J. Biochem.*, **222**, 1055-1061.
6. Suzuki, A., Yoshida, M., Hayashi, K., Mizuno, Y., Hagiwara, Y. and Ozawa, E. (1994) Molecular organization at the glycoprotein complex binding site of dystrophin. *Eur. J. Biochem.*, **220**, 283-292.
7. Jung, D., Yang, B., Meyer, J., Chamberlain, J.S. and Campbell, K.P. (1995) Identification and characterization of the dystrophin anchoring site on  $\beta$ -dystroglycan. *J. Biol. Chem.*, **270**, 27305-27310.
8. Ervasti, J.M. and Campbell, K.P. (1993) A role for the dystrophin-glycoprotein complex as a transmembrane linker between laminin and actin. *J. Cell Biol.*, **122**, 809-823.
9. Campbell, K.P. (1995) Three muscular dystrophies: loss of cytoskeleton-extracellular matrix linkage. *Cell*, **80**, 675-679.
10. Ohlendeick, K., Ervasti, J.M., Matsumura, K., Kahl, S.D., Leveille, C.J. and Campbell, K.P. (1991) Dystrophin related protein is localized to neuromuscular junction of adult skeletal muscle. *Neuron*, **7**, 499-508.
11. Bowe, M.A., Deyst, K.A., Leszyk, J.D. and Fallon, J.F. (1994) Identification and purification of an agrin receptor from Torpedo post-synaptic membranes: a heteromeric complex related to the dystroglycans. *Neuron*, **12**, 1171-1180.
12. Campanelli, J.T., Roberds, S.L., Campbell, K.P. and Scheller, S.H. (1994) A role for dystrophin-associated glycoproteins for and utrophin in agrin-induced AChR clustering. *Cell*, **77**, 663-674.
13. Gee, S.H., Montanaro, F., Lindenbaum, M.H. and Carbonetto, S. (1994) Dystroglycan- $\alpha$ , a dystrophin-associated glycoprotein is a functional agrin receptor. *Cell*, **77**, 675-686.

14. Sugiyama, J., Bowen, D.C. and Hall, Z.W. (1994) Dystroglycan binds nerve and muscle agrin. *Neuron*, **13**, 103–115.
15. Gesemann, M., Cavalli, V., Denzer, A.J., Brancaccio, A., Schumacher, B. and Rugg, M.A. (1996) Alternative splicing of agrin alters its binding to heparin, dystroglycan, and the putative agrin receptor. *Neuron*, **16**, 755–767.
16. Tian, M., Jacobsen, C., Gee, S.H., Campbell, K.P., Carbonetto, S. and Jucker, M. (1996) Dystroglycan in the cerebellum is a laminin  $\alpha$ 2-chain binding protein at the glial-vascular interface and is expressed in Purkinje cells. *Eur. J. Neurosci.* **8**, 2739–2747.
17. Durbejj, M., Larsson, E., Ibragimov-Beskrovnaya, O., Roberds, S.L., Campbell, K.P. and Ekblom, P. (1995) Non-muscle  $\alpha$ -dystroglycan is involved in epithelial development. *J. Cell Biol.*, **130**, 79–91.
18. Schofield, J.N., Górecki, D.C., Blake, D.J., Davies, K. and Edwards, Y.H. (1995) Dystroglycan mRNA expression in normal and mdx mouse embryogenesis: a comparison with utrophin and apo-dystrophins. *Dev. Dynamics*, **204**, 178–185.
19. Yotsumoto, S., Fujiwara, H., Horton, J.H., Mosby, T.A., Wang, X., Cui, Y. and Ko, M.S.H. (1996) Cloning and expression analyses of mouse dystroglycan gene: specific expression in maternal decidua at the peri-implantation stage. *Hum. Mol. Genet.*, **5**, 1259–1267.
20. Leivo, I., Vaheri, A., Timpl, R. and Wartiovaara, J. (1980) Appearance and distribution of collagens and laminin in the early mouse embryo. *Dev. Biol.*, **76**, 100–114.
21. Lin, T.-P., Labosky, P.A., Grabel, L.B., Kozak, C.A., Pitman, J.L., Kleeman, J. and MacLeod, C.C. (1994) The *Pem* homeobox gene is X-linked and exclusively expressed in extraembryonic tissues during early murine development. *Dev. Biol.*, **166**, 170–179.
22. Jollie, W.P. (1968) Changes in the fine structure of the parietal yolk sac of the rat placenta with increasing gestational age. *Am. J. Anat.*, **122**, 513–532.
23. Jensen, M., Koszalka, T.R. and Brent, R.L. (1975) Production of congenital malformations using tissue antisera. *Dev. Biol.*, **42**, 1–12.
24. Coucouvanis, E. and Martin, G.R. (1995) Signals for death and survival: A two-step mechanism for cavitation in the vertebrate embryo. *Cell*, **83**, 279–287.
25. Clark, C.C., Tomicheck, E.A., Koszalka, T.R., Minor, R.R. and Kefalides, N.A. (1975) The embryonic rat parietal yolk sac. *J. Biol. Chem.*, **250**, 5259–5267.
26. Hogan, B.L.M., Cooper, A.R. and Kurkinen, M. (1980) Incorporation into Reichert's membrane of laminin-like extracellular proteins synthesized by parietal endoderm cells of the mouse embryo. *Dev. Biol.*, **80**, 289–300.
27. Kadoya, Y., Kadoya, K., Durbejj, M., Holmval, K., Sorokin, L. and Ekblom, P. (1995) Antibodies against domain E3 of laminin-1 and integrin  $\alpha$ 6 subunit perturb branching epithelial morphogenesis of submandibular gland, but by different modes. *J. Cell Biol.*, **129**, 521–534.
28. Fox, J.W., Mayer, U., Nischt, R., Aumailley, M., Reinhardt, D., Weidemann, H., Mann, K., Timpl, R., Kreig, T., Engel, J. and Chu, M.-L. (1991) Recombinant nidogen consists of three globular domains and mediates binding of laminin to collagen type IV. *EMBO J.*, **10**, 3137–3146.
29. DeArchangelis, A., Neuville, P., Boukamel, P., Lefebvre, O., Kedinger, M. and Simon-Assmann, P. (1996) Inhibition of laminin  $\alpha$ 1-chain expression leads to alteration of basement membrane assembly and cell differentiation. *J. Cell Biol.*, **133**, 417–430.
30. Ohlendeick, K., Matsumura, K., Ionasescu, V.V., Towbin, J.A., Bosch, E.P., Weinstein, S.L., Sernett, S.W. and Campbell, K.P. (1993) Duchenne muscular dystrophy: deficiency of dystrophin-associated proteins in the sarcolemma. *Neurology*, **43**, 795–800.
31. Roberds, S.L., Ervasti, J.M., Anderson, R.D., Ohlendeick, K., Kahl, S.D., Zoloto, D. and Campbell, K.P. (1993) Disruption of the dystrophin-glycoprotein complex in the cardiomyopathic hamster. *J. Biol. Chem.*, **268**, 11496–11499.
32. Helbling-Leclerc, A., Zhang, X., Topaloglu, H., Cruaud, C., Tesson, F., Weissenbach, J., Tome, F.M., Schwartz, K., Fardeau, M., Trygvasson, K. and Guicheney, P. (1995) Mutations in the laminin  $\alpha$ 2-chain gene (LAMA2) cause merosin-deficient congenital muscular dystrophy. *Nature Genet.*, **11**, 216–218.
33. Jobsis, G.J., Keizers, H., Vreijling, J.P., deVisser, M., Speer, M.C., Wolterman, R.A., Baas, F. and P.A. Bolhuis. (1996) Type VI collagen mutations in Bethlem myopathy, an autosomal dominant myopathy with contractures. *Nature Genet.*, **14**, 113–115.
34. Nagy, A., Rossant, J., Nagy, R., Abramow-Newerly, W. and Roder, J.C. (1993) Derivation of completely cell culture-derived mice from early-passage embryonic stem cells. *Proc. Natl. Acad. Sci. USA*, **90**, 8424–8428.
35. Ervasti, J.M. and Campbell, K.P. (1991) Membrane organization of the dystrophin-glycoprotein complex. *Cell*, **66**, 1121–1131.
36. Durham, P.L. and Snyder, J.M. (1995) Characterization of  $\alpha$ 1,  $\beta$ 1, and  $\gamma$ 1 laminin subunits during rabbit fetal lung development. *Develop. Dyn.*, **203**, 408–421.